RMP Colloquia

Independent particle motion and correlations in fermion systems

Vijay R. Pandharipande

Department of Physics, University of Illinois, Urbana, Illinois 61801

Ingo Sick

Department of Physics and Astronomy, Universität Basel, CH-4056 Basel, Switzerland

Peter K. A. deWitt Huberts

NIKHEF-K, NL 1009AJ Amsterdam, The Netherlands

The independent-particle model explains many features of atomic nuclei and other fermion systems. The low-energy states of nearly closed-shell systems can be interpreted as having *quasiparticles* in single-particle orbitals. The difference between physical particles and quasiparticles results from the effects of correlations in the system. In this Colloquium the authors consider the consequences of these correlations. They discuss in particular, mainly for the case of nuclei, the quasihole strength z (spectroscopic factor) that gives the probability of the quasiparticle's being a physical particle. Results from both theory and experiment indicate that $z \sim 0.65$ and imply that only $\sim 2/3$ of the time a nucleon acts as an independent particle bound in an average potential. The fraction of $\sim 1/3$ of correlated nucleons is larger than believed in the past. [S0034-6861(97)00703-4]

CONTENTS

I. INTRODUCTION

Historically, the notion of independent particle motion was first introduced to describe the structure of atoms and explains the periodic table of the elements. In its most naive form the shell model assumes that the electrons in an atom occupy single-particle orbitals that are eigenstates of an average potential created by the Coulomb interaction of the electrons with the atomic nucleus and with each other. The Hartree-Fock theory (Hartree, 1928; Fock, 1930), based on this assumption, is remarkably accurate in describing the noble-gas atoms. For example, the binding energies of neon and argon atoms, calculated with the Hartree-Fock approximation and bare Coulomb force (Clementi and Roetti, 1974), differ by only 0.2% from the exact ground-state eigenvalues (Veillard and Clementi, 1968) of the nonrelativistic many-body Schrödinger equation.

The first insights on *nuclear* structure were provided by the liquid-drop model (Bethe and Bacher, 1936; von Weizsäcker, 1935). It pictured nuclei as drops of charged, incompressible, liquid nuclear matter and explained nuclear binding energies as sums of volume, surface, and Coulomb terms. The nucleons in nuclei were regarded as strongly interacting with each other, a view based on Bohr's compound nucleus model of nuclear reactions (Bohr, 1936) in which the incident neutrons's energy is assumed to dissipate totally via collisions with nucleons in the nucleus. However, many nuclear properties, such as the existence of magic nuclei with extra stability like that of rare-gas atoms, spins and parities of nuclear ground states, and the existence of deformed nuclei, were unexplained. The success of the nuclear shell model (Haxel *et al.*, 1949; Mayer, 1949) in explaining these properties surprised many physicists (Weidenmüller, 1990). Historically, the shell model became accepted primarily on the basis of a detailed and successful comparison with the observed ground-state properties (spin, parity) and excitations at low energy. Today, the shell model has become the basis upon which most model calculations of nuclear structure rely.

The successes of the liquid-drop and compound-nucleus models had been interpreted as evidence against collisionless single-particle motion assumed in the shell model. Does the success of the shell model really "prove" that nucleons do move independently in a fully occupied Fermi sea as assumed in Hartree-Fock approaches? In fact, it was soon realized that single-particle motion can persist at low energies in fermion

 0034-6861/97/69(3)/981(12)/$11.80

systems due to the suppression of collisions by Pauli exclusion. The compound-nucleus reactions occur at relatively high excitation energies where many collisions are not Pauli blocked. Fermi-liquid theory (Landau, 1957a, 1957b), based on related ideas, was developed in 1957. It showed that strongly interacting systems can resemble in many aspects a noninteracting Fermi gas, but with quasiparticles as constituents. These quasiparticles have properties such as effective mass and effective interactions which differ from those of the bare particles; these effective properties can compensate to a fair degree for the lack of correlations in the model wave function.

Another system recently discovered to exhibit independent particle motion and shell structure is a *cluster of metal atoms* (Brack, 1993; de Heer, 1993). Here the ionic metal cores provide a uniformly charged background in a finite volume, and the valence electrons, which are strongly delocalized with a wave function that extends over the whole cluster, represent the quantal system that exhibits shell structure. The mean field seen by the electrons corresponds to a potential that closely resembles the Woods-Saxon shape familiar from nuclear physics, but with rather small surface diffuseness. This system presents many direct analogies to nuclei, the major difference being the smallness of the spin-orbit force. Magic numbers 2, 8, 20, etc. have been observed, up to values above 3000. These metal clusters allow a very nice extension of the shell model and indicate a major new feature that goes beyond those observed in other quantal systems subject to a mean-field description: the appearance of supershells. The usual shell structure of the level density is modulated with a periodicity of $\simeq 1000$ atoms. This supershell structure results from the transition to the semiclassical regime appropriate for systems with many constituents. It can be understood as an interference between the two most important classical closed trajectories in a spherical cavity with reflecting walls, the ones forming a triangle and a square. The shell effects in metal clusters provide a means to study the transition of finite fermion systems from the atomic to the mesoscopic and perhaps even macroscopic dimension.

Besides systems such as atoms, nuclei, and metallic clusters, the phenomenon of quantum shell structure is also predicted to occur in small drops of atomic Fermi-liquid ^{3}He (Lewart *et al.*, 1988). We note that even in strongly interacting Bose liquids, atomic liquid ^{4}He for example, single-particle motion manifests itself in the form of a condensate at low temperature. Thus the role played by the Pauli principle, though large in Fermi systems, is not essential for having a fraction of particles moving freely in quantum liquids. In drops of the Bose liquid ^{4}He atoms are predicted to condense into the $1s$ orbital. Recent comparative studies (Moroni *et al.*, 1997) have indicated interesting similarities in the single-particle properties of Bose and Fermi quantum liquids.

In the nuclear shell model, the nucleons occupy eigenstates of a single-particle potential generated by interparticle interactions. Hartree-Fock calculations based on effective interactions (Negele, 1982), or energy-density functionals (Dechargé and Gogny, 1980) succeed in reproducing the observed shell structure and binding energies fairly accurately. However, unlike in atoms, the Hartree-Fock approximation cannot be used with *realistic* interactions to describe even the simplest closed-shell nuclei or atomic ^{3}He liquid drops.

In atomic helium liquids the two-particle distribution function $g(r)$, which gives the probability of finding two particles at a distance r apart, is known (Svensson *et al.*, 1980) to have a hole at small r created by the repulsive core in the interatomic potential. The $g(r)$ in nuclei is not that well established experimentally; it is predicted to have a rich spin-isospin-dependent structure with toroidal, dumbbell, and spherical shapes (Forest *et al.*, 1996) reflecting the intricacies of nuclear forces. These short-range correlations, missing in the mean-field approximation, are essential for the binding of the system. They represent the collisions between particles which lead to virtual excitations and fractional occupation of single-particle orbitals. Those which have unit occupation in the naive picture have relatively large occupation probabilities close to one, while others that are empty in Hartree-Fock have small, but >0, occupations. In a paper commenting on the work of Bertsch and Kuo (1968), G. Brown (1969) conjectured that depletions (the difference between unity and the occupation probability) of the Fermi sea as large as 40% might occur in nuclei. The empirical evidence at that time seemed to indicate, however, very small depletions.

The consequences of correlations are difficult to measure and to calculate. Only during the last few years has it become possible to observe effects of the deviation of occupation numbers from 0 or 1 and thus obtain quantitative information on the limits of the naive shell model. In this Colloquium we review in some detail the case of the nucleus, and discuss, in particular, results of electron-nucleus scattering experiments which probe the shape and occupation probabilities of single-particle orbitals in nuclei.

II. SHELL MODEL FOR THE NUCLEAR INTERIOR?

The surprise about the success of the nuclear shell model concerns the fact that independent particle motion could occur in a system that has a density as high as the one occurring on average in nuclei and with interactions as strong as the nucleon-nucleon interaction. This success might come as a lesser surprise, perhaps, once one realizes that much of the knowledge on nuclei concerns *surface* properties. Even the most integral quantities, such as calculated energy eigenvalues, are weighed with r^2; experimental spectroscopic observables like spectroscopic factors are completely dominated by the low-density surface region.

The domination of low nuclear densities in experimental observables is directly related to the strong absorption of nuclear projectiles in the nucleus. This absorption is particularly pronounced for composite projectiles (ejectiles) such as d, ^{3}He used traditionally in single-nucleon transfer reactions to obtain spectroscopic

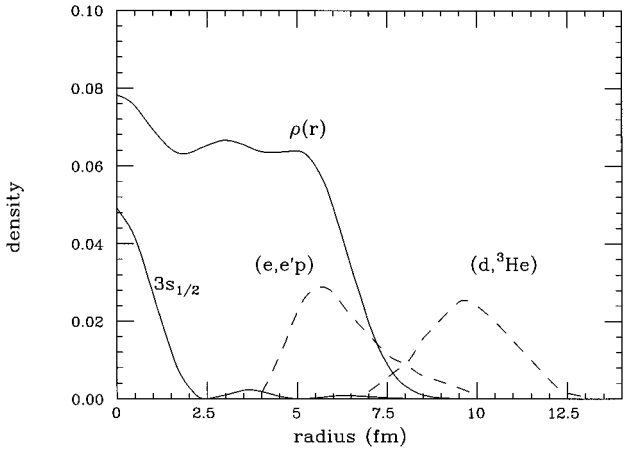

FIG. 1. Radial sensitivity of one-nucleon transfer reactions used to study nucleon wave functions (dashed lines), compared to density of Pb and the 3*s* shell. The radial sensitivity of (e,e) is independent of r.

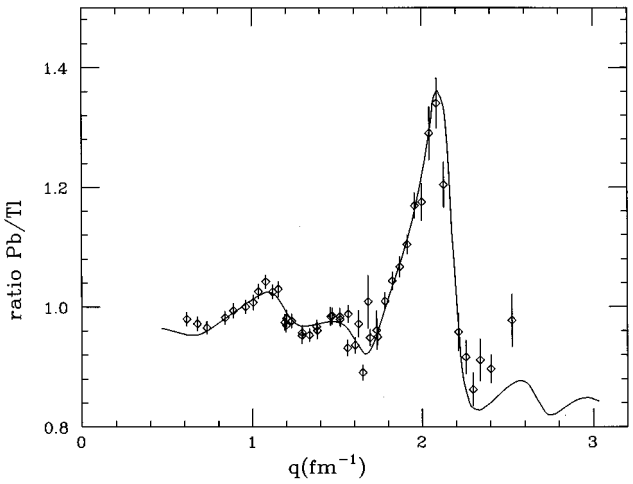

FIG. 2. Ratio of ^{206}Pb- to ^{205}Tl-elastic electron scattering cross sections, together with prediction from shell-model calculation with adjusted occupation number. The peak at 2 fm^{-1} results from the Fourier transform of the 3*s* proton radial wave function, which resembles a damped oscillation. The amplitude of the peak yields the difference in occupation of the 3*s* shell between ^{206}Pb and ^{205}Tl (see text).

information. The absorption in the nuclear interior is strong and the maximal sensitivity to bound-state wave functions occurs at radii where the density has fallen to less than one tenth of the density in the interior (see Fig. 1). Much of the experimental information on spectroscopic properties, then, concerns the asymptotic normalization of wave functions and hardly relates to the high-density interior.

The surface domination is enhanced by a feature that is intrinsic to a finite system of fermions. The least-bound shells—the ones experimentally studied in typical nuclear reactions—also have high angular momenta; only in rare cases do the states near the Fermi edge have low l. High-l states have a radial wave function that peaks in the nuclear surface region, and much of any integral over $R_l(r)$ comes from the lower-density region of the nucleus.

Is it then true that the shell model offers a valid approach for the description of nuclei, or does the model appear to be successful only because many observables are ''superficial?''

In order genuinely to gauge the validity of the independent-particle description, one needs to consider observables that are sensitive to the nuclear interior, i.e., observables measured with probes that are not absorbed when interacting with the nucleus. At the same time, one needs probes that allow one to achieve good spatial resolution, in order to differentiate between the nuclear surface and the interior. Observables accessible via electron scattering at large momentum transfer offer the best (and perhaps only) tool.

Experiments on elastic (e,e) scattering have provided us with detailed measurements of the density in the nuclear interior; densities as accurate as 1% have been measured in selected cases (Sick *et al.*, 1975, 1979; Frois *et al.*, 1977; Cavedon *et al.*, 1982). They have been compared to Hartree-Fock calculations done using finite-range effective nucleon-nucleon interactions derived from nucleon-nucleon scattering. This comparison shows important differences despite the fact that the effective interactions have been tuned to reproduce the *average* density in the nuclear interior. The calculated densities exhibit oscillatory structure that results from building up the density from the radial wave functions of the individual shells, and this structure is much more pronounced than in the experimental densities. This disagreement already points to a partial occupation of the shell-model states, or a different shape of the orbitals in the nuclear interior.

The most convincing test of the validity of the shell model in the nuclear interior comes from a precise measurement of the density difference of ^{206}Pb and ^{205}Tl. In the shell model these nuclei differ by a 3*s* proton. The 3*s* shell has a very distinct radial wave function, with a maximum at $r=0$, with 2 nodes and two further maxima (see Fig. 1). This radial wave function can easily be distinguished from all other shells, and it has a unique signature in the cross-section ratios between ^{205}Tl and ^{206}Pb. The experiment of Cavedon *et al.* (1982) showed that this 3*s* radial wave function is indeed a reality, even in the very center of the lead nucleus (Figs. 2, 3). A 3*s* radial wave function as calculated in a shell-model approach, but with modified occupation (see Sec. III.B), perfectly explains the data. In the nuclear interior the *shape* of the orbits as predicted by the independent-particle model seems to be realistic!

Orbitals with properties close to the ones predicted by the shell model are not only found for states near the Fermi edge. Already the early $(e,e'p)$ work (Mougey *et al.*, 1976) indicated that deeply bound nucleons have momentum distributions similar to those predicted by the independent-particle model.

From this observation we learn that the shape of the single-particle wave functions—be it in radial or mo-

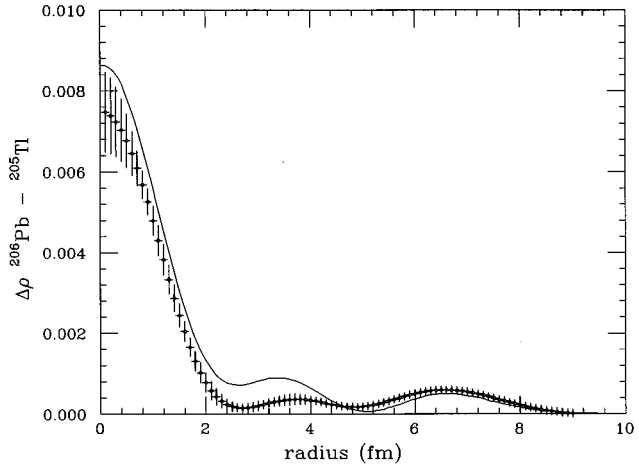

FIG. 3. Density difference between ^{206}Pb and ^{205}Tl. The experimental result of Cavendon *et al.* (1982) is given by the error bars; the prediction obtained using Hartree-Fock orbitals with adjusted occupation numbers is given by the curve. The systematic shift of 0.0008 fm^{-3} at $r \leqslant 4$ fm is due to deficiencies of the calculation in predicting the core polarization effect.

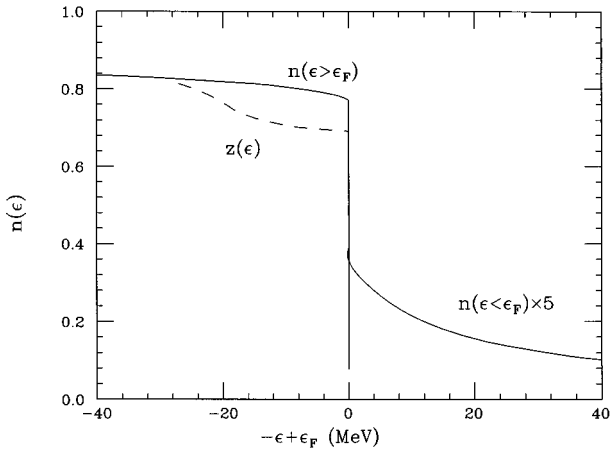

FIG. 4. Occupation of states of nuclear matter as a function of ε, with ε_F referring to the Fermi energy. The dashed curve gives the quasihole strength z.

mentum space—is quite close to the one predicted by a single-particle calculation. The most telling information on deviations from the shell model is found in the occupation numbers. These quantities therefore assume a particular place in our discussion.

III. THEORY

We next discuss the various concepts of *orbitals* in correlated systems and the calculated occupation probabilities. We first address the case of an infinite Fermi liquid of constant density, which is easier to discuss than finite systems. This allows us to introduce the concepts of the spectral function and the renormalization function $z(k)$. We then discuss the various types of orbitals that are relevant for finite systems. For both types of systems we shall use theoretical results for both nuclear and atomic systems to illustrate the concepts.

A. Nuclear matter

We begin the theoretical discussion with idealized infinite nuclear matter representing the ground state of matter in the absence of the Coulomb force, which puts a limit on the size of nuclei. Gross properties of large nuclei, such as binding energies, size, etc., can be easily understood by regarding them as charged drops of nuclear matter. At low temperatures nuclear matter is expected to be a superfluid; however, the shell gaps in single-particle energies are larger than the pairing gap in nuclei, and hence pairing is believed to be unimportant in the closed-shell nuclei considered here. Therefore we shall regard nuclear matter as a normal Fermi liquid and ignore its superfluid properties.

The single-particle orbitals in nuclear matter are plane-wave eigenstates of the momentum, due to translational invariance, which simplifies the theory considerably. The one-body density matrix is diagonal in these states, whose occupation numbers give the momentum distribution $n(k)$ of nucleons in nuclear matter. The momentum distribution $n(k)$ has been calculated for realistic nuclear forces with the correlated basis-functions (CBF) method (Fantoni and Pandharipande, 1984) as well as with the Brueckner-Bethe-Goldstone (BBG) method (Dickhoff and Muther, 1992). The results for $n(k)$ obtained with the CBF method and the Urbana model of the nucleon-nucleon force are shown in Fig. 4 using the single-particle spectrum $\varepsilon(k)$.

Due to correlations, the occupation number $n(k<k_F)$ for momenta below the Fermi momentum k_F is reduced to 0.7–0.8, and the states with $k>k_F$ have small but finite occupations. Atomic liquid ^{3}He, another Fermi liquid, has been extensively studied. Its predicted $n(k)$ (Fabrocini *et al.*, 1992) is shown in Fig. 5 for comparison. Because of the large repulsive core in the interatomic potential, the $n(k<k_F)$ in liquid ^{3}He is expect-

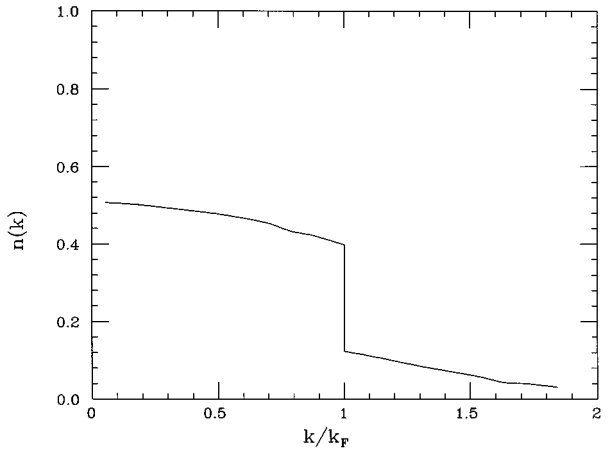

FIG. 5. Momentum distribution of atomic ^{3}He liquid at the experimental equilibrium density.

ed to be only 0.4. The repulsive core in the internucleon potential is relatively smaller; much of the depletion of the $n(k<k_F)$ in nuclear matter is believed to be due to the strong tensor force between nucleons (Fantoni and Pandharipande, 1984). This should be compared to the case of a ''good shell-model system,'' such as one of the noble-gas atoms; for neon, the occupation numbers differ from unity by 0.001–0.009 only, while for argon the difference is 0.002–0.018, increasing from the innermost to the outermost shell (Jungen, 1996).

The removal spectral function $P_h(k,E)$, defined by

$$P_h(k,E)=\sum_I |\langle I|a_k|0\rangle|^2 \delta(E_I-E_0-E), \tag{1}$$

where E_0 is the energy of the nuclear matter in its ground state $|0\rangle$, the E_I indicate the energies of the states $|I\rangle$ having one nucleon less, and a_k is the annihilation operator, gives the probability density that the residual system will be in states with energy $E+E_0$ upon removing a nucleon of momentum k. It contains much more information than the $n(k)$ given by its integral:

$$n(k)=\int_{-E_F}^{\infty} P_h(k,E)dE. \tag{2}$$

For example, if we could either neglect or subtract the effects of the final-state interactions of the struck nucleon, the missing energy spectrum in an $(e,e'p)$ reaction on nuclear matter is given by $P_h(k,E)$ at missing momentum k.

The $P_h(k,E)$ has also been calculated for realistic nuclear forces using the CBF (Benhar *et al.*, 1989) and BBG (Dickhoff and Muther, 1992) methods, and typical results are shown in Fig. 6. At $k<k_F$ it has a ''quasihole'' peak at $E>-\varepsilon_F$ superimposed on a broad background, while at $k>k_F$ it has a broad background centered at $\simeq k^2/2m$. In contrast $P_h(k>k_F)=0$ and $P_h(k<k_F)=\delta(E+k^2/2m)$ in an ideal Fermi gas. The quasihole peak becomes very sharp as k approaches k_F from below, and the integrated strength in it is denoted by the ''renormalization function'' $z(k)$. This peak represents Landau's quasihole in a quantum liquid, and it has been shown (Migdal, 1957) that

$$z(k=k_F)=(n(k_F-\epsilon)-n(k_F+\epsilon))_{\epsilon\to+0}. \tag{3}$$

The values of $z(k)$ obtained (Benhar *et al.*, 1989) with the CBF method are shown in Fig. 4.

Quasiparticles having $k>k_F$ can be similarly defined using the spectral function with an $a_k^\dagger$ in place of a_k in

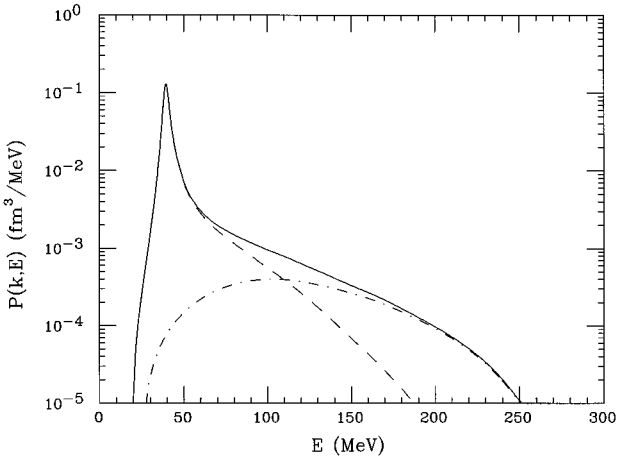

FIG. 6. Nuclear matter spectral function at a fixed nucleon momentum $k/k_F=0.75$: dashed curves, uncorrelated parts; dot-dashed curves, correlated parts.

Eq. (1). Quasiparticles or holes with k close to k_F have long lifetimes; therefore at low temperatures Fermi liquids exhibit independent quasiparticle motion. The presence of correlations generated by the strong interparticle interactions is reflected by the deviation of $z(k)$ from unity as well as by the increase in the widths of the quasihole and particle peaks as k deviates from k_F. The z gives the probability of the quasiparticle's being a physical particle. The correlated particles account for all of the $n(k>k_F)$, and they also contribute to the $n(k<k_F)$. Therefore $z(k)<n(k)$. In the strongly correlated atomic liquid ^{3}He the $z(k=k_F)$ is predicted to be only about 0.3, while that for nuclear matter is about 0.7.

B. Finite nuclei

A similar analysis for finite systems (nuclei, Fermi-liquid drops) is more complex because their single-particle orbitals, unlike plane waves, are not uniquely determined by symmetry. The occupation numbers are eigenvalues of the one-body density matrix, whose eigenfunctions are called *natural orbitals* (Löwdin, 1955) and denoted here by $\phi_{n,ljm}$. We do not discuss these natural orbitals further as they are not directly related to observable quantities. The removal spectral function has a more natural representation in *overlap orbitals* denoted by $\psi_{i,ljm}$. These are defined from the overlap of the A-nucleon ground state Ψ_A and the states $\Psi_{A-1,i}$ of $(A-1)$ nucleons having $J,M=j,-m$,

$$\psi_{i,ljm}(x_A)=\int \Psi^\dagger_{A-1,i}(x_1,\ldots,x_{A-1})\Psi_A(x_1,\ldots,x_A)dx_1\cdots dx_{A-1}, \tag{4}$$

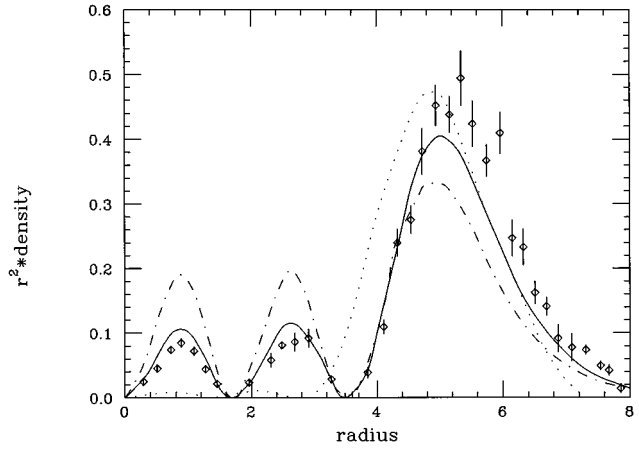

FIG. 7. 3*s* orbitals: dotted curve, natural orbital; dot-dashed curve, mean-field orbital; solid curve, local-density approximation for quasihole orbital. The points represent the calculated quasihole orbital.

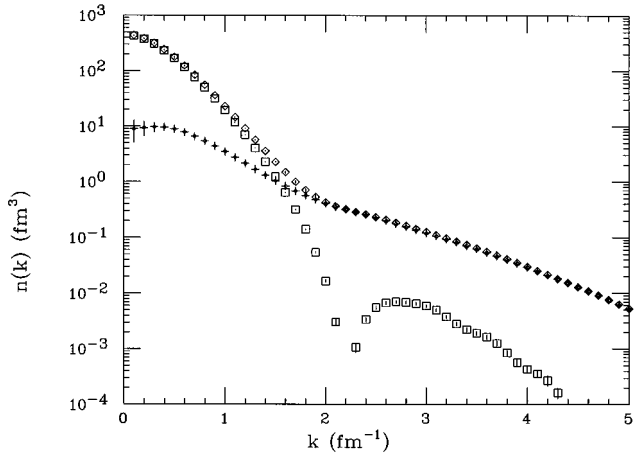

FIG. 8. Variational Monte Carlo result for momentum distributions in ^{4}He: ($\diamond$), total momentum distribution; ($\square$), quasihole; (+), difference.

where x_A denotes the position, spin, and isospin of the nucleon A. Theories of finite fermion systems are more complex because the various $\psi_{i,ljm}$ are generally not orthogonal to each other. Only in the absence of correlations, i.e., in the Hartree-Fock approximation, do both the natural orbitals and the overlap orbitals equal the Hartree-Fock orbitals $\xi_{n,ljm}$, and considerable simplification occurs. Even in the presence of correlations there are a few low-energy states, one for each l,j, for which the norm of the overlap orbital $\psi_{i,ljm}$ is close to unity. We refer to these states as quasihole states, and their norm, generally called the spectroscopic factor, as the quasihole normalization z.

As for infinite systems, correlations also lead to an increase of the width of the more deeply bound quasihole states as observed in $(e,e'p)$ (Quint, 1987a; Leuschner, 1994). Given the fact that much of this increase is due to coupling to surface excitations (Rijsdijk *et al.*, 1992), the spreading is more difficult to exploit quantitatively, in terms of short-range correlations, than are the z values.

C. Calculated results

It is difficult to calculate the eigenstates of finite fermion systems with strong interparticle interactions. However, for liquid ^{3}He drops the interatomic force is a simple spin-independent function of the distance between the atoms, and therefore variational Monte Carlo (VMC) calculations with correlated wave functions are easily possible (Lewart *et al.*, 1988). Their accuracy is limited by that of the variational wave function, which includes two- and three-body spatial correlations. Wave functions including such correlations successfully describe many properties of the bulk liquid. The orbitals of a 70-atom drop have been studied in detail (Lewart *et al.*, 1988). The 70 atoms occupy the same shells as the protons in ^{208}Pb, the additional 12 protons in lead are in the $1h_{11/2}$ state, lowered because of the spin-orbit splitting (which is absent in the atomic ^{3}He liquid drop).

The overlap orbital, calculated from the overlaps of the 69- and 70-atom ground states, is called the $3s_{1/2}$ quasihole orbital and is shown in Fig. 7 along with other approximations. Finally a potential well $V(r)$ can be defined such that the density of 70 noninteracting atoms in this well equals that of the 70-atom drop. The single-particle orbitals in this well are considered as the *mean-field orbitals* $\xi_{n,ljm}$, and the $3s$ mean-field orbital is shown in Fig. 7. Simple, approximate relations between the mean-field orbitals and the natural orbitals and quasihole orbitals can be derived (Lewart *et al.*, 1988). In particular the local-density approximation,

$$\psi(r) \simeq \sqrt{z(\rho(r))}\,\xi(r), \tag{5}$$

where $z(k_F,\rho)$ is the renormalization constant for uniform liquid at density ρ, seems to reproduce the quasihole orbital calculated from variational wave functions containing interparticle correlations. However, these wave functions do not contain effects of the coupling of the quasiparticles to the surface of the drop.

Because of the strong spin-isospin dependence of the nuclear force, quantum Monte Carlo calculations for nuclei are much more difficult. Thus far, exact calculations have been possible only for nuclei with up to 7 nucleons (Pudliner, 1996), including the doubly magic nucleus ^{4}He. The $1s_{1/2}$ quasihole orbital obtained from the overlap of ^{4}He and ^{3}H is shown in Fig. 8 along with the total momentum distribution $n(k)$ of protons in ^{4}He. These results have been obtained (Wiringa, 1996) using modern models of the nuclear force. The normalization z of the quasihole orbital is 0.81, while that of $n(k)$ is unity. At small k almost the entire momentum distribution is explained by the quasihole orbital, while at large k the quasihole orbital contributes little to $n(k)$. In heavier nuclei we also expect that nucleons with small momenta would come mostly from the quasihole orbitals, while those with large k come from correlations. The spectral function of nucleons with large k will be peaked at

$E \simeq k^2/2m_N$, with m_n the nucleon mass, like that in nuclear matter.

In studies of Fermi systems, liquid ^{3}He and nuclei offer complementary opportunities. Measurement of pair distribution functions are simpler for the extended liquid, while for nuclei $(e,e'p)$ and (e,e) experiments allow a direct measurement of z and the density distributions of quasiparticle states.

Quantum Monte Carlo calculations (Lewart *et al.*, 1988) indicate that particles in Bose liquid drops condense in an orbital given by $\psi_0(r) = \sqrt{n_c(\rho(r))}\xi_0(r)$, where $\xi_0(r)$ is the lowest mean-field orbital and $n_c(\rho)$ is the fraction of particles condensed in the liquid at density ρ. Here $n_c(\rho)$ plays the role of $z(\rho)$ in Eq. (5), and ψ_0 approximates the quasihole orbital obtained from overlaps of Bose ground states.

It is important to realize that the momentum distribution of these quasihole orbitals at large k falls very quickly, as do those of mean-field orbitals and the data for low removal energies (Bobeldijk *et al.*, 1995). The tail to large k shown in Fig. 8 is connected nearly exclusively to states of large removal energy.

Recent diffusion Monte Carlo calculations (Moroni *et al.*, 1997) of liquid ^{3}He and ^{4}He have provided additional insight into the role played by the Pauli principle. To a good approximation, the density matrix of liquid ^{3}He factorizes into the one calculated for bosonic ^{3}He and the Fermi-gas Slater function, and the z factor of fermionic ^{3}He almost coincides with the condensate fraction of the mass-3 bosonic liquid. This shows that the quenching of occupation is essentially bosonic in nature and is largely decoupled from the additional effects of Pauli exclusion.

IV. SPECTROSCOPIC STRENGTH FROM EXPERIMENT

We next demonstrate that there exists a convincing body of empirical evidence, derived primarily from electron scattering experiments, in support of z values of 0.6–0.7 for quantum states that are near the Fermi surface of closed-shell nuclei. We consider the following cases: (i) Quasielastic knockout of protons by high-energy electrons, from which the spectral function can be derived; (ii) charge-density differences between pairs of isotones, from which, when combined with relative spectroscopic factors, absolute occupation numbers can be derived; (iii) elastic and inelastic form factors of high multipolarity. In the concluding section we reconsider single-nucleon transfer reactions that employ the radial wave functions derived from electron scattering and take stock of the internal consistency of the results from the various approaches.

A. z factors from $(e,e'p)$

In the quasifree $(e,e'p)$ reaction, where the scattered electron is detected in coincidence with the knocked-out proton, the initial momentum k and energy E of the proton can be reconstructed and the spectral function $S(k,E)$ determined.

In plane-wave impulse approximation (PWIA) the cross section for a given E reads

$$\sigma = K\sigma_{ep}\psi_h^2(k)z, \tag{6}$$

where K is a kinematic factor, σ_{ep} is the off-shell electron-proton scattering cross section, $\Psi_h(k)$ is the quasihole orbital normalized to one, and z is the quasiparticle normalization factor. With a spectrometer pair with 1:10 000 energy resolution and the use of dispersion-matching techniques (de Vries *et al.*, 1984) the $(e,e'p)$ reaction has been systematically studied with a missing-mass resolution of 100 keV. With electron energies of the order of 500 MeV, three-momentum transfers of the order of 400 MeV/c and energy transfers of 100–150 MeV could be achieved (van der Steenhoven and de Witt Huberts, 1991).

The experimental conditions employed were such that the reaction dynamics could be treated with confidence using the distorted-wave impulse approximation (DWIA), which accounts for both the Coulomb distortion of the electron and the strong interaction effects experienced by the proton (Boffi *et al.*, 1993; McDermott, 1990). The latter process is treated using an optical potential with parameters fixed by fits to elastic proton-nucleus scattering data. The adequacy of the optical-potential approximation seems convincingly demonstrated by the correct description of the complicated shape of the experimental momentum distribution for many valence-hole orbitals studied throughout the periodic table (Lapikás, 1993). Coupled-channel effects have been studied both theoretically and experimentally and appear to be small for strong knockout channels. Extensive tests for data obtained in a variety of kinematic conditions (different kinematics, range of proton energies) indicate that the variance of the z factor deduced from $A(e,e'p)A-1$ amounts to typically 5–10%.

We shall discuss below three representative examples, z factors obtained for the doubly magic nuclei ^{4}He, ^{16}O, and ^{208}Pb.

For *helium* the $1s_{1/2}$ quasihole orbital can be accurately calculated with Monte Carlo methods and realistic ^{4}He and ^{3}H wave functions. The calculation (Schiavilla *et al.*, 1986) used the Urbana V_{14} N-N potential supplemented with a phenomenological three-body force and yielded a $z = 0.8$. Differential cross sections for the ^{4}He $(e,e'p)^3$H reaction have been calculated (Laget, 1994) in a microscopic model including the effects of the final-state interaction and the coupling of the virtual photon to proton, neutron, and meson currents. As shown in Fig. 9 the results calculated from the quasihole orbital match the data, with better than 10% accuracy, in the momentum range up to 230 MeV/c, above which final-state interactions and meson current effects dominate. This result indicates that N-N correlations are indispensable for a realistic description of the electrodisintegration of ^{4}He.

An additional piece of evidence is derived from the spectral function at large k and E values that has been recently measured (Leeuwe, 1995). The high-momentum components resulting from the short-range

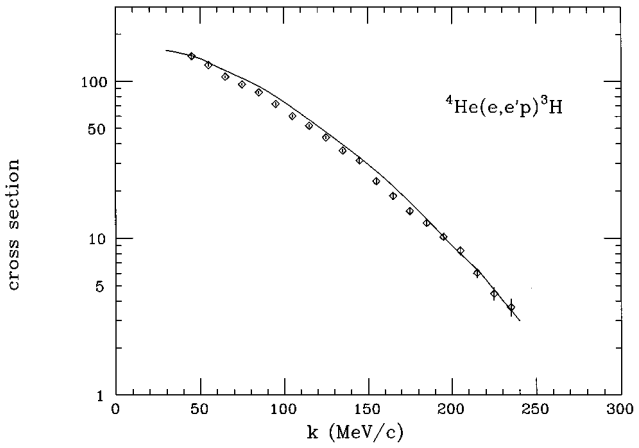

FIG. 9. Cross sections for ^{4}He (Leeuwe, 1995), compared to calculation (Laget, 1994) using variational Monte Carlo wave function with z=0.8.

N-N interaction are correlated in the spectral function with large values of E. Absorption of a virtual photon on such a correlated pair leads to a broad structure in the cross section with a maximum at $E=k^2/2m$. The measurements of the spectral function for values up to $k=600$ MeV/c and $E=100$ MeV demonstrate the existence of such a structure with the predicted kinematic behavior and constitute a direct proof of correlations in ^{4}He. See Fig. 10.

The shell structure of *oxygen* is of particular interest because the spin-orbit partners $1p_{1/2}$ and $1p_{3/2}$ are well separated in energy (6 MeV) and the knockout spectrum shows the spectroscopic strength concentrated in the ^{15}N ground state and the excited state $J=3/2$ at 6 MeV. Angular momentum analysis of the spectral function up to 20 MeV shows less than 10% additional $l=1$ strength (Leuschner, 1994). For the $p_{1/2}$ state, which is not fragmented, z=0.63.

For the doubly magic nucleus ^{208}Pb the $(e,e'p)$ data (Quint, 1987a, 1987b; Lapikás, 1993) have been analyzed

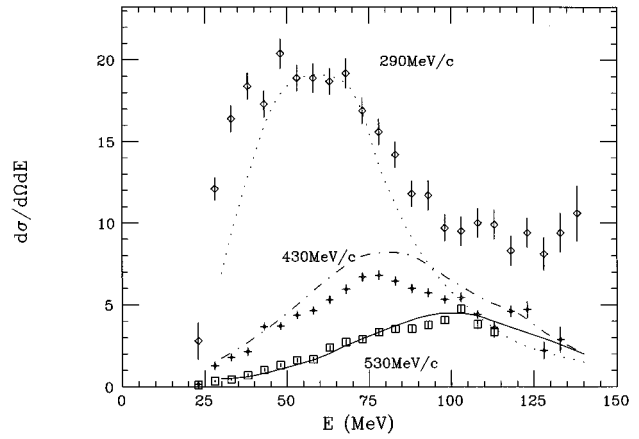

FIG. 10. Cross section for ^{4}He$(e,e'p)$ [roughly proportional to $S(k,E)$] as function of E, for several values of k. Both data and calculation (Leeuwe, 1995) show the peak expected to occur at $E\simeq k^2/2m_N$.

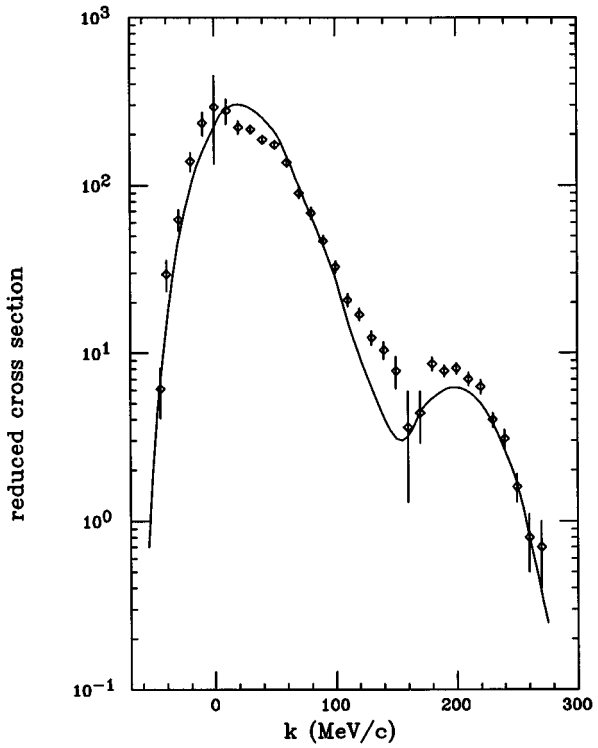

FIG. 11. Distorted momentum distribution of the 3s state in ^{208}Pb, experiment (Quint, 1987a) and calculation (McDermott, 1990) using a shell-model momentum distribution with adjusted z.

with a full phase-shift treatment of the distortion induced both by the Coulomb interaction acting on the electron and the strong interaction experienced by the knocked-out proton (McDermott, 1990; Jin *et al.*, 1994). The result for the transition to the ground state of ^{207}Tl is shown in Fig. 11.

The shape appears to be well reproduced in the k range up to 100 MeV/c. The slight deviations at large values of k from the theoretical shape are quite interesting, since they signal a deviation of the overlap wave function from the mean-field shape in the interior of ^{208}Pb. This region of the momentum was therefore not included in the procedure to extract z.

The spectral function for $l=0$ quantum states is large at low values of the momentum where the spectral function of $l\neq 0$ states is small. This provides a powerful tool to detect $l=0$ strength at larger excitation energies. All of the low-energy $l=0$ spectroscopic strength in ^{208}Pb is found to be located in the ground state; up to 20 MeV, no additional strength is found.

The ground-state spectroscopic strength gives $z=0.68\pm 0.06$ for the 3s orbital. This is the key result for this prototype quasihole orbital in the heavy doubly magic nucleus ^{208}Pb. The value is remarkably low considering that for several decades values near one were assumed.

A relativistic mean-field approximation has also been developed for closed-shell nuclei like ^{16}O and ^{208}Pb, which contain many nucleons (Serot, 1992). Both bound

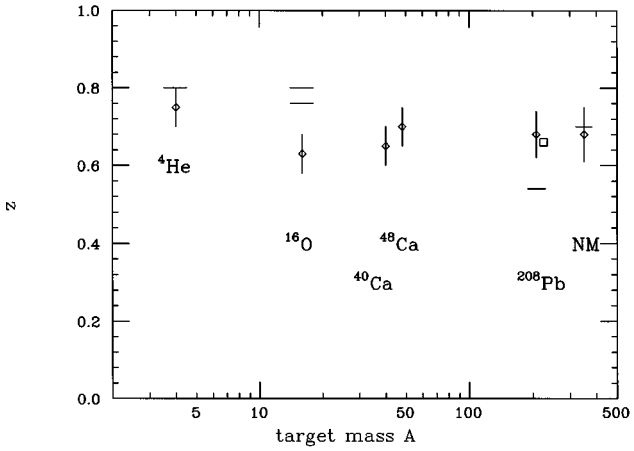

FIG. 12. z factors ($\diamond$) from $(e,e'p)$ and (e,e') reactions; ($\square$), from optical potential analysis; and from (—) theory.

and continuum orbitals are described with Dirac wave functions. Analysis of the $(e,e'p)$ data within this approach yields values for z that are not significantly different from those obtained using nonrelativistic wave functions.

We now summarize the experimental findings in Fig. 12. The z factors are systematically quenched and exhibit a large reduction relative to the Hartree Fock (shell-model) value of one. Figure 12 also shows results of theoretical calculations using variational wave functions (Schiavilla *et al.*, 1986; Benhar *et al.*, 1990; Radichi *et al.*, 1994) for ^{4}He, ^{16}O, and nuclear matter. These wave functions are known to be very accurate for ^{3}H and ^{4}He, while they neglect the possible coupling of single-particle motion to the nuclear surface for the heavier nuclei. The observed value of z in ^{208}Pb has been explained by adding surface effects to the nuclear matter result (Benhar *et al.*, 1990).

Figure 12 also shows the value of z (Mahaux and Sartor, 1989) derived by exploiting the analytic properties of the optical potential (and integral quantities thereof) to extrapolate from the positive energies accessible in proton-nucleus scattering to the negative energies (bound states). From the potential they derive spectroscopic factors and occupation numbers of single-particle states. Also shown is the value for oxygen (Geurts *et al.*, 1996) calculated using the Green's-function formalism.

The $(e,e'p)$ experiments have had a pronounced impact in our appreciation of the occupation of single-particle states. We note in this context that a similar tool, the $(e,2e)$ reaction, has also become a useful tool for the study of atoms and molecules (McCarthy and Weigold, 1991; Vos and McCarthy, 1995). These $(e,2e)$ experiments have a somewhat different focus, however, as the attention is mainly directed towards momentum distributions. Spectroscopic factors come in only when discussing the (long-range) correlations occurring in molecules.

B. Occupation numbers

As pointed out above, $(e,e'p)$ has set new standards in the measurement of the momentum distributions and spectroscopic factors of nucleons in nuclei. These momentum distributions can be understood largely in terms of the shell model. The data show that these spectroscopic factors differ from unity by substantial amounts.

While $(e,e'p)$ has removed many of the limitations affecting the one-nucleon transfer reactions used in the past, the method still runs into difficulties when aiming at occupation numbers. One could have hoped that occupation numbers of shell-model orbitals could be obtained by summing the spectroscopic strength associated with the removal of a nucleon from a specific n,l,j orbital. In practice this is very difficult; the strength of interest is spread very thinly over a large range of E and is difficult to identify due to the continuum nature of the residual nuclear states involved. Moreover, at large excitation energies the strength of many n,l,j orbitals with different radial quantum numbers n can be mixed. In principle the overlap orbital for each state of the residual nucleus is a different superposition of the natural orbitals.

An approach (Clement *et al.*, 1987) that combines results from elastic electron scattering and $(e,e'p)$ provides a way to estimate the occupation number of the quasihole orbital. It is applicable in particular to the nuclei near lead, where the needed (e,e) data are available. ^{208}Pb is also the most interesting case, as this heavy "doubly magic" nucleus represents the prototype case for which one would like to know the degree to which the shell model is valid.

We have discussed above the (e,e) data that provided the precise information on the $3s$ quasihole orbital in the interior of ^{206}Pb (see Sec. II). The charge-density difference between ^{205}Tl and ^{206}Pb is given by

$$\Delta\rho(r)=\sum_{\alpha}\Delta n_{\alpha}\cdot\rho_{\alpha}(r)+\Delta\rho_{cp}(r), \tag{7}$$

where n_α and ρ_α are the occupation numbers and single-particle radial densities of states α. $\Delta\rho_{cp}=\Sigma_\alpha n_\alpha\Delta\rho_\alpha$ is a small correction that reflects the fact that all $\rho_\alpha(r)$ are slightly changing when going from nucleus $(A-1)$ to nucleus A. The quantity $\Delta n^{206}=n_{3s}^{206}-n_{3s}^{205}$ can be obtained from the unique signature of the $3s$ radial wave function in elastic electron scattering and is found to be 0.64 ± 0.06 (Sick and de Witt Huberts, 1991).

Denoting the spectroscopic factor of various states for removal of the $3s$ protons in ^{208}Pb by s_{3s}^{208}, and using $n_{3s}^{208}=\Sigma s_{3s}^{208}$, one obtains the trivial identity

$$n_{3s}^{208}=\Delta n_{3s}^{206}\Big/\left(\frac{\Sigma s_{3s}^{206}}{\Sigma s_{3s}^{208}}-\frac{\Sigma s_{3s}^{205}}{\Sigma s_{3s}^{208}}\right). \tag{8}$$

In this equation, only *ratios* of sums of spectroscopic factors occur. The spectroscopic factors are known only for low energy discrete states which appear to have overlap functions proportional to the QHO. We denote their sum Σ'. The spread of the strength over a large range in excitation energy, due to the short-range repulsion in the nucleon-nucleon interaction, can be expected to be very similar for neighboring nuclei. When taking *ratios* of terms involving sums over s values, one may

expect that the fraction of the strength which has moved to high excitation energy drops out. In the above equation one thus may replace the sum Σ which extends to infinite excitation energy by the sum Σ' that covers only the discrete states. These Σ' terms *can* be extracted from spectroscopic factors measured by $(e,e'p)$.

The combination of data from elastic electron scattering and $(e,e'p)$ data then leads (Sick and de Witt Huberts, 1991) to an absolute occupation probability of the $3s$ state—the prototype example for a state near the Fermi edge in a magic nucleus—of 0.76 ± 0.07. A direct comparison between the absolute occupation probability and the $(e,e'p)$ results for spectroscopic factors is only possible after adding some theoretical input (Pandharipande *et al.*, 1984). This gives a difference of occupation number and spectroscopic factor of 0.14. Augmenting the $(e,e'p)$ strength by this yields 0.82 ± 0.08, in good agreement with the occupation of 0.76 ± 0.07.

C. High-Λ form factors

A number of other types of observables have been considered in the past to get information on spectroscopic factors of single-particle states. We mention elastic magnetic form factors of multipolarity $\Lambda=2j$ for the case of an even-odd nucleus with the unpaired nucleon in the orbit having $j=l+1/2$, particularly for cases in which the valence nucleon has the largest j value of all normally occupied states (Platchkov *et al.*, 1982). As long as one ignores admixtures to the ground-state wave function with $j'>j$, the overall amplitude of the $M\Lambda$ form factor is related by a sum rule (Dieperink and Sick, 1982) to sums over spectroscopic factors involving the shell j. Shells with $j'<j$ cannot contribute to multipolarity Λ.

Today, we realize that the strength outside the shell-model space is spread over a large range in energy and, as a consequence, is spread over many values of j, mostly with $j'>j$. The contribution of transitions between states with $j'_1+j'_2\geqslant 2j$ leads to a background contribution that invalidates the simple sum rule cited above. The sum rule could be exploited if the background contribution could be subtracted based on the different q dependence of the corresponding form factor. This for the time being is not practical, however, given the limited set of data available for these $M\Lambda$ form factors.

Similar considerations hold for the inelastic $E\Lambda$ or $M\Lambda$ form factors (Pandharipande *et al.*, 1984). Background contributions have to be subtracted to extract the value of z from these data. The z values from $(e,e'p)$ are more accurate because no such subtractions are needed.

D. Spectroscopic factors from transfer reactions

Historically, one-nucleon transfer reactions provided the most solid empirical foundation for the validity of the shell model. The spectroscopic factors deduced from transfer reactions were persistently in the range 0.9–1.0, i.e., close to the independent-particle limit for a closed shell. The much lower z factors obtained today from the proton knockout data call for an explanation.

In the early literature (MacFarlane, 1969) it was clearly understood that the extraction of absolute spectroscopic factors from single-nucleon transfer reactions is highly model dependent, the principal reason being that the cross section is extremely sensitive to the Ansatz for the wave function of the transferred nucleon. The reaction amplitude samples the asymptotic part of the wave function at large distance r from the nuclear center, where ψ_h^2 is down by a factor of 100 from its maximum value. The cross section changes by typically 10% for a change of 1% of the radius R of the potential well used to calculate the bound-state wave function. The failure to find significant hole strength in the excitation energy range then accessible (5–10 MeV) led the practitioners of single-nucleon transfer reactions to choose implicitly a value for R that would exhaust the $(2j+1)$ particle+hole sum rule.

Today one can use the information on the rms radius of the quasihole wave function deduced from $(e,e'p)$ in order to reduce the model dependence of the transfer reaction analysis. A sample of pickup reactions $(d,{}^3\mathrm{He})$ has been reanalyzed (Kramer, 1990; Kramer *et al.*, 1997). The average z factor for the doubly magic nuclei oxygen, calcium, and lead amounts to 0.62 ± 0.15, a value that agrees with the z factors from $(e,e'p)$. We are thus arriving at a rather consistent picture presented by two totally different types of reactions.

V. "MISSING" STRENGTH

A significant measurement of the absolute occupation probabilities of normally occupied states below the Fermi level is difficult, precisely because of the relative success of the shell model. The occupation probabilities n are not all that far from 1, and the significance of a measurement lies in the uncertainty of the *difference* from unity. Given the systematic errors of n, the relative error on $(1-n)$ may become very large.

Alternatively, one can try to measure the hole strength below the Fermi level or the particle strength above it. The integral over either would yield the information on the deviation of n from 1 directly.

Historically, a great deal of effort has been spent in nuclear physics on measurements of spectroscopic factors via one-nucleon transfer reactions (see previous section). These experiments found very little strength in the region of excitation energy up to $\simeq$10 MeV. From this the conclusion was drawn that the *integrated strength*—the quantity that yields the occupation numbers above E_F and their deviation from unity below E_F—is small. The nuclear shell model, with occupation probabilities very close to 1, seemed to be valid.

The ultimate failure of these attempts lies in the limitation to excitation energies of the order of 10 MeV, i.e., energies at which the strength of well-defined l,j can be identified because of the discrete nature of the residual

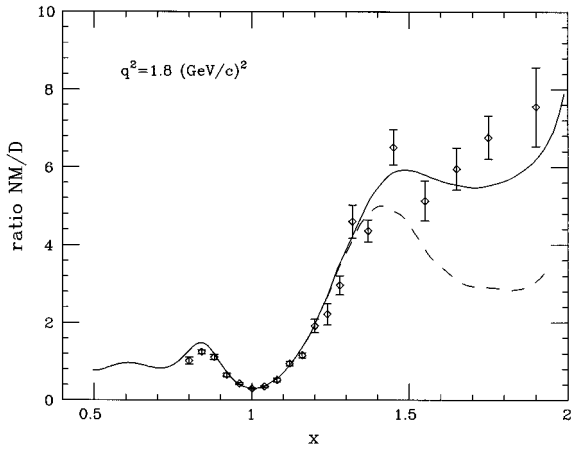

FIG. 13. Ratios of inclusive cross sections of nuclear matter and deuterium at 3.6 GeV and 25° as a function of the Bjorken scaling variable $x=q^2/2m_N\omega$. The solid curve corresponds to the prediction using the correlated basis-functions spectral function (Benhar *et al.*, 1995). For the dashed curve the strength in the spectral function at large momentum has been reduced by a factor of 2 to show the sensitivity of the data to components of high momentum.

nuclear states. In doubly closed-shell nuclei only a fraction $z\sim0.65$ of the hole strength is located in this energy region. The rest, which includes the fraction $n-z\sim0.1$ of the hole strength and all of the particle strength, populates two-hole/one-particle and more complex excitations. In nuclei of interest, these excitations are mostly in the continuum region.

Access to the elusive particle strength at high k,E, is possible when using inclusive scattering of a weakly interacting probe, in the kinematical region of large momentum transfer q. This type of approach has been employed both in the study of liquid helium, using neutron scattering, and in the investigation of nuclei, using electron scattering. In the tail of the quasielastic peak observed in (n,n') or (e,e') the cross section is sensitive to the strength at large k,E.

This sensitivity of the tail of the quasielastic peak was known for some time, but could not be exploited for lack of a quantitative treatment of the final-state interaction of the knocked-out nucleon. The recent development of Correlated Glauber Theory for the quantitative treatment of the final-state interaction (Benhar *et al.*, 1991) allows us to estimate the total particle strength for $k>k_F$. The study of the ratios of the cross section for infinite nuclear matter [obtained by extrapolating data for nuclei (Day *et al.*, 1989)] to deuterium has recently provided us with a good number on the integral over this strength (Benhar *et al.*, 1995). In the region $1.5<x<2$, where the ratio is nearly proportional to the momentum density at large k, it has been shown that, within the uncertainty of $\simeq20\%$, the strength agrees with the value of $\simeq0.25$ predicted by CBF theory for nuclear matter (see Fig. 13).

When discussing these measurements, it may be instructive to look again at other cases in which correlations lead to strength at large k,E. For the case of Bose liquid helium, much of the interest in the past had been focused on small k, in connection with the Bose condensate. Only recently have neutron scattering experiments on Fermi liquid ^{3}He (Azuah *et al.*, 1995) been carried out in the region of q,ω appropriate for a study of the tail of the quasielastic peak. The statistical errors on the data are still fairly large in the tail, but the data seem to indicate that almost 50% of the ^{3}He atoms occupy states with momenta $k>k_F$.

VI. CONCLUSIONS

The independent-particle model has provided a very economical description and has allowed us to understand many features of nuclei. Yet this model must fail in certain areas, given the internucleon correlations resulting from the repulsive core and the tensor part of the nucleon-nucleon interaction. The experimental and theoretical work of the past decade has provided us with a much clearer picture on the consequences of these correlations. In particular, it has become clear that the main consequences are a depletion of the occupation of orbits that are fully occupied in the shell model and a spreading of this strength over an extremely wide range of excitation energies. The quantitative information we have today from both theory and experiment tells us that occupation probabilities in finite nuclei are only in the 75% range. Single-particle contributions to transitions are suppressed by the factor z, which amounts to 0.65. Thus at any time only 2/3 of the nucleons in the nucleus act as independent particles moving in the nuclear mean field. The remaining third of the nucleons are correlated.

The depopulation of states below the Fermi energy is much more pronounced than was believed in the past. In the future, one clearly would like to use a model that accounts for this fact, preferably without giving up the shell model entirely. Modern Monte Carlo approaches retain both the quasiparticle and correlated aspects, but the economy and simplicity of the shell model is lost. One of the challenges for the future will be to find simpler methods that allow one to treat simultaneously the uncorrelated and the correlated nucleons in the nucleus.

For experiment, one of the challenges will be the investigation of the deeply bound shell-model states in the heavier nuclei and the identification of the correlated strength of the spectral function at large momentum and energy.

ACKNOWLEDGMENTS

The authors want to thank A. E. L. Dieperink, T. W. Donnelly, S. Fantoni, M. N. Harakeh, C. Mahaux, B. Mottelson, and R. Wiringa for helpful discussions and critical advice.

REFERENCES

Azuah, R., W. Stirling, K. Guckelsberger, R. Scherm, S. Bennington, M. Yates, and A. Taylor, 1995, J. Low Temp. Phys. **101,** 951.

Benhar, O., A. Fabrocini, and S. Fantoni, 1989, Nucl. Phys. A **505,** 267.

Benhar, O., A. Fabrocini, and S. Fantoni, 1990, Phys. Rev. C **41,** 24.

Benhar, O., A. Fabrocini, S. Fantoni, G. Miller, V. Pandharipande, and I. Sick, 1991, Phys. Rev. C **44,** 2328.

Benhar, O., A. Fabrocini, S. Fantoni, and I. Sick, 1995, Phys. Lett. B **343,** 47.

Bertsch, G., and T. Kuo, 1968, Nucl. Phys. A **112,** 204.

Bethe, H., and R. Bacher, 1936, Rev. Mod. Phys. **8,** 82.

Bobeldijk, I. B., *et al.*, 1995, Phys. Lett. B **356,** 13.

Boffi, S., C. Giusti, and F. Pacati, 1993, Phys. Rep. **226,** 1.

Bohr, N., 1936, Nature (London) **137,** 344.

Brack, M., 1993, Rev. Mod. Phys. **65,** 677.

Brown, G., 1969, Comments Nucl. Part. Phys. **3,** 136.

Cavedon, J., B. Frois, D. Goutte, M. Huet, P. Leconte, C. Papanicolas, X.-H. Phan, S. Platchkov, S. Williamson, W. Boeglin, and I. Sick, 1982, Phys. Rev. Lett. **49,** 978.

Cavedon, J., J. Bellicard, B. Frois, D. Goutte, M. Huet, P. Leconte, P. Ho, S. Platchkov, and I. Sick, 1982, Phys. Lett. B **118,** 311.

Clement, H., P. Grabmayr, H. Roehm, and G. Wagner, 1987, Phys. Lett. B **183,** 127.

Clementi, E., and A. Roetti, 1974, At. Data Nucl. Data Tables **14,** 177.

Day, D., J. McCarthy, Z. Meziani, R. Minehart, R. Sealock, S. Thornton, J. Jourdan, I. Sick, B. Filippone, R. McKeown, R. Milner, D. Potterveld, and Z. Szalata, 1989, Phys. Rev. C **40,** 1011.

de Heer, W., 1993, Rev. Mod. Phys. **65,** 611.

de Vries, C., C. de Jager, L. Lapikas, G. Luijckx, R. Maas, H. de Vries, and P. de Witt Huberts, 1984, Nucl. Instrum. Methods Phys. Res. A **223,** 1.

Dechargé, J., and D. Gogny, 1980, Phys. Rev. C **21,** 1568.

Dickhoff, W., and H. Muther, 1992, Rep. Prog. Phys. **55,** 1947.

Dieperink, A., and I. Sick, 1982, Phys. Lett. B **109,** 1.

Fabrocini, A., V. Pandharipande, and Q. Usmani, 1992, Nuovo Cimento A **14,** 469.

Fantoni, S., and V. Pandharipande, 1984, Nucl. Phys. A **427,** 473.

Fock, V., 1930, Z. Phys. **61,** 126.

Forest, J., V. Pandharipande, S. Pieper, R. Wiringa, R. Schiavilla, and A. Arriaga, 1996, Phys. Rev. C **54,** 646.

Frois, B., J. Bellicard, J. Cavedon, M. Huet, P. Leconte, P. Ludeau, A. Nakada, P. X. Hô, and I. Sick, 1977, Phys. Rev. Lett. **38,** 152.

Geurts, W., K. Allaart, W. Dickhoff, and H. Müther, 1996, Phys. Rev. C **53,** 2207.

Hartree, D. R., 1928, Proc. Camb. Philos. Soc. **24,** 89.

Haxel, O., J. Jensen, and H. Suess, 1949, Phys. Rev. **75,** 1766.

Jin, Y., D. Onley, and L. Wright, 1994, Phys. Rev. C **50,** 168.

Jungen, M., 1996, private communication.

Kramer, G., H. Blok, and L. Lapikas, 1997, unpublished.

Kramer, G. J., 1990, Ph.D. thesis (University of Amsterdam).

Laget, J., 1994, Nucl. Phys. A **579,** 333.

Landau, L., 1957a, Sov. Phys. JETP **3,** 920.

Landau, L., 1957b, Sov. Phys. JETP **5,** 101.

Lapikás, L., 1993, Nucl. Phys. A **553,** 297c.

Leeuwe, V. 1995, Ph.D. thesis (University of Amsterdam).

Leuschner, M., 1994, Phys. Rev. C **49,** 955.

Lewart, D., V. Pandharipande, and S. Pieper, 1988, Phys. Rev. B **37,** 4950.

Löwdin, P., 1955, Phys. Rev. **97,** 1474.

MacFarlane, M., 1969, in *Proceedings of the International Conference on Nuclear Structure*, edited by M. Harvey, R. Y. Cusson, J. S. Geiger, and J. M. Pearson (Les Presses de l'Université de Montreal, Montreal), p. 385.

Mahaux, C., and R. Sartor, 1989, Nucl. Phys. A **493,** 157.

Mayer, M., 1949, Phys. Rev. **75,** 1969.

McCarthy, I. E., and E. Weigold, 1991, Rep. Prog. Phys. **54,** 789.

McDermott, J.P., 1990, Phys. Rev. Lett. **65,** 1991.

Migdal, A., 1957, Sov. Phys. JETP **5,** 333.

Moroni, S., G. Senatore, and S. Fantoni, 1997, Phys. Rev. B **55,** 1040.

Mougey, J., M. Bernheim, A. Bussière, A. Gillebert, P. X. Ho, M. Priou, D. Royer, I. Sick, and G. Wagner, 1976, Nucl. Phys. A **262,** 461.

Negele, J., 1982, Rev. Mod. Phys. **54,** 913.

Pandharipande, V., C. Papanicolas, and J. Wambach, 1984, Phys. Rev. Lett. **53,** 1133.

Platchkov, S., J. Bellicard, J. M. Cavedon, B. Frois, D. Goutte, M. Huet, P. Leconte, P. Xuan-Ho, P. de Witt Huberts, and L. Lapikás, 1982, Phys. Rev. C **25,** 2318.

Pudliner, S., 1996, Ph.D. thesis (University of Illinois).

Quint, E., 1987a, Phys. Rev. Lett. **58,** 1088.

Quint, E., 1987b, Ph.D. thesis (University of Amsterdam).

Radichi, M., S. Boffi, S. C. Pieper, and V. Pandharipande, 1994, Phys. Rev. C **50,** 3010.

Rijsdijk, G., K. Allaart, and W. H. Dickhoff, 1992, Nucl. Phys. A **550,** 159.

Schiavilla, R., V. Pandharipande, and R. Wiringa, 1986, Nucl. Phys. A **449,** 219.

Serot, B., 1992, Rep. Prog. Phys. **55,** 1947.

Sick, I., and P. de Witt Huberts, 1991, Comments Nucl. Part. Phys. **20,** 177.

Sick, I., J. Bellicard, J. Cavedon, B. Frois, M. Huet, P. Leconte, P. Ho, and S. Platchkov, 1979, Phys. Lett. B **88,** 240.

Sick, I., J. Bellicard, M. Bernheim, B. Frois, M. Huet, P. Leconte, J. Mougey, P. X. Ho, D. Royer, and S. Turck, 1975, Phys. Rev. Lett. **35,** 910.

Svensson, E., V. Sears, A. Woods, and P. Martel, 1980, Phys. Rev. B **21,** 3638.

van der Steenhoven, G., and P. de Witt Huberts, 1991, in *Modern Topics in Electron Scattering*, edited by B. Frois and I. Sick (World Scientific, Singapore), p. 510.

Veillard, A., and A. Clementi, 1968, J. Chem. Phys. **49,** 2415.

von Weizsäcker, C., 1935, Z. Phys. **96,** 431.

Vos, M., and I. McCarthy, 1995, Rev. Mod. Phys. **67,** 713.

Weidenmüller, H., 1990, Nucl. Phys. A **507,** 5c.

Wiringa, R., 1996, private communication.